Sub-Persistence-Length Complex Scaling Behavior in Lysozyme Amyloid Fibrils

Cécile Lara, Ivan Usov, Jozef Adamcik, and Raffaele Mezzenga*

ETH Zurich, Food & Soft Materials Science, Institute of Food, Nutrition & Health, Schmelzbergstrasse 9, LFO E23, 8092 Zurich, Switzerland

(Received 18 March 2011; published 28 November 2011)

We combine atomic force microscopy single-molecule analysis with polymer physics concepts to study molecular conformations of lysozyme amyloid fibrils. We resolve a wavy structure of the fibrils in which the scaling behavior varies at multiple length scales. Bond and pair correlation functions, end-to-end distribution, and wormlike chain model identify three characteristic length scales. At short length scales (≈ 150 nm), there is a first bending transition of the fibrils corresponding to a bending length L_b. At larger length scales ($> 2L_b$), fibrils become pseudoperiodic and start to undulate. Finally, at length scales larger than the persistence length ($\sim \mu$m), the fibrils become flexible and follow a 2D self-avoiding random walk. We interpret these results in terms of the twisting of the fibrils and the impact this has on the area moment of inertia and the propensity of the fibril to bend.

DOI: 10.1103/PhysRevLett.107.238101 PACS numbers: 87.14.em, 36.20.Ey, 87.64.Dz

Proteins unfolding and self-assembly in the form of amyloid aggregates has primary significance in the fields of medicine, biology, food, and material science due to their implication in neurodegenerative diseases [1,2], their mechanical characteristics [3], and texture building properties [4]. Their ability to form supramolecular aggregates *in vivo* or *in vitro* suggests a common tendency of proteins and polypeptides to form amyloids [5].

Lysozyme, which is prone to fibrillation both *in vivo* and *in vitro*, is responsible for systemic amyloidosis [6]. Hen egg white lysozyme (HEWL), whose structure is highly homologous to human lysozyme, can also form amyloid fibrils *in vitro* and can cause cell death under specific conditions [7,8]. Although HEWL fibrillation has been extensively studied [9,10], no reports have tackled systematically the molecular configurations at various length scales, spanning from the fibril cross section to its contour length.

Atomic force microscopy (AFM) allows extracting structural information of single macromolecules and biopolymers at high resolution. When combined with a statistical polymer physics analysis, this technique has probed to successfully describe molecular conformations of biological polyelectrolytes such as DNA [11,12] or structural properties of amyloid fibrils such as in β-lactoglobulin [13–15].

In general, the first crucial concept by which biomacromolecules can be classified is the scaling exponent [16,17]. However, contrary to regular fractals, which are self-similar on all length scales, polymers and biomacromolecules are random fractals whose behavior depends on the length scale considered. Below the persistence length L_p, polymers have a rodlike behavior whereas above L_p, their fractal dimension depends on the molecular interactions and the space dimension considered: in two dimensions, an ideal random walk (RW) maintains a fractal exponent of 2 while a self-avoiding random walk (SAW) has a lower exponent of $4/3$. Within the same dimensionality limit, the average end-to-end distance $\langle R(s)\rangle$ of a polymer of contour length s scales as $\langle R(s)\rangle \sim s^{\nu}$, in which ν is the reciprocal of the fractal exponent. Thus, in real polymers, rodlike to RW transition is observed only at one single length scale corresponding to L_p.

In the present Letter we show that, under controlled denaturation conditions of high temperature and low pH, lysozyme forms a nontrivial type of amyloid fibrils which cannot be defined by a single L_p and whose description requires as many as three characteristic length scales. While the fibrils are well described by a SAW at length scales larger than the persistence length ($\sim \mu$m), the rodlike behavior below L_p is disrupted by a characteristic undulating periodicity that appears at lower length scales ($P \approx 250$ nm), which can be used to model the fibril as a pseudosinusoid. At even lower length scales ($< P/2$), called bending length scale, the fibrils become rodlike again and recover a one-dimensional behavior. We show that different scaling regimes apply, when spanning these characteristic length scales from large to small, with a progressive change in the scaling exponent following $4/3 \rightarrow 1 \rightarrow x \rightarrow 1$, where x is a number slightly larger than 1 reflecting the nonlinearity of the pseudosinusoid at the length scale of an undulation period, and we revisit these findings in terms of periodic height fluctuations along the amyloid fibrils. The biological relevance of such a wavy structure is confirmed by its recent identification in disease-related amyloid fibrils isolated from amyloidotic organs (Asp67His lysozyme) or from prion cells [18,19].

Amyloid fibrils were prepared by incubation of 2% w/w HEWL at pH 2 and 60 °C for several days. Data for this work were acquired by tapping mode AFM on dry samples prepared with 20 μl aliquots diluted to 0.1% w/w with pH

2 Milli-Q water, deposited onto freshly cleaved mica or graphite, incubated for 2 min, rinsed, and dried, to study the conformation of lysozyme amyloids adsorbed on the substrate. Cryogenic and room-temperature transmission electron microscopy were also employed in order to rule out potential substrate-induced artifacts on the conformations of the amyloid fibrils.

Since amyloid fibrils are semiflexible biopolymers, whose flexibility can be described by their persistence length L_p [13,20,21] one expects to distinguish two scaling exponents: below L_p the fibrils should behave as rigid rods ($\nu = 1$) and for $s \gg L_p$ they should obey SAW theory (since L_p is several orders of magnitude larger than the Debye length, electrostatic effects can be neglected).

In Fig. 1, the $\langle R(s)\rangle$ versus s of 66 amyloid fibrils, as the one shown in the inset, is plotted for s ranging from the pixel size (3 nm) to the total contour length of the fibrils (~ 20 μm). The limiting slopes at low and high s, provide the ν exponents at low and high length scales, respectively. As expected, in the limit of low length scales a slope of 0.99 is found, indicating rodlike behavior, whereas at larger length scale a slope of 0.75 is found, as expected for a 2D SAW ($\nu = 3/4$), consistent with the observations made for single-stranded or circular DNA adsorbed on a surface [11,22]. Fitting of the bond correlation function provides an average $L_p \approx 2.5$ μm.

However, at higher resolution of the fibril, short-scale periodic undulations become visible (Fig. 1, right inset) which are not accounted for by the coarser analysis shown in Fig. 1. Most of the wavy fibrils are less than 4 nm thick and have a period of about 250 nm (Supplemental Material, Fig. S1 [23]) independent of the pH to which they are postexposed (Fig. S2 [23]): Fig. 2(a) shows the cryo-TEM imaging of these fibrils, which being exempt from potential substrate artifacts, confirms in bulk the same characteristic undulating shape and periods observed by AFM (Fig. S3 [23]). In Figs. 2(b) and 2(c) the undulations have been resolved sufficiently well to be reflected in the characteristic exponent ν. A real fibril (pointed by white arrow in

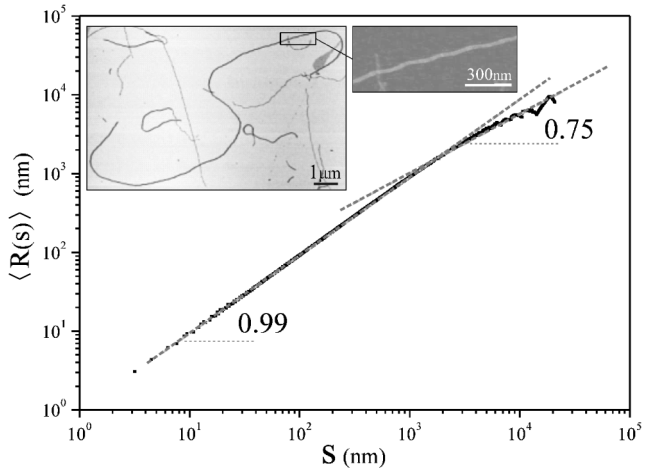

FIG. 1. Mean internal end-to-end distance $\langle R(s)\rangle$ versus contour length s. The AFM height image of a representative lysozyme amyloid fibril and its high magnification are depicted as insets.

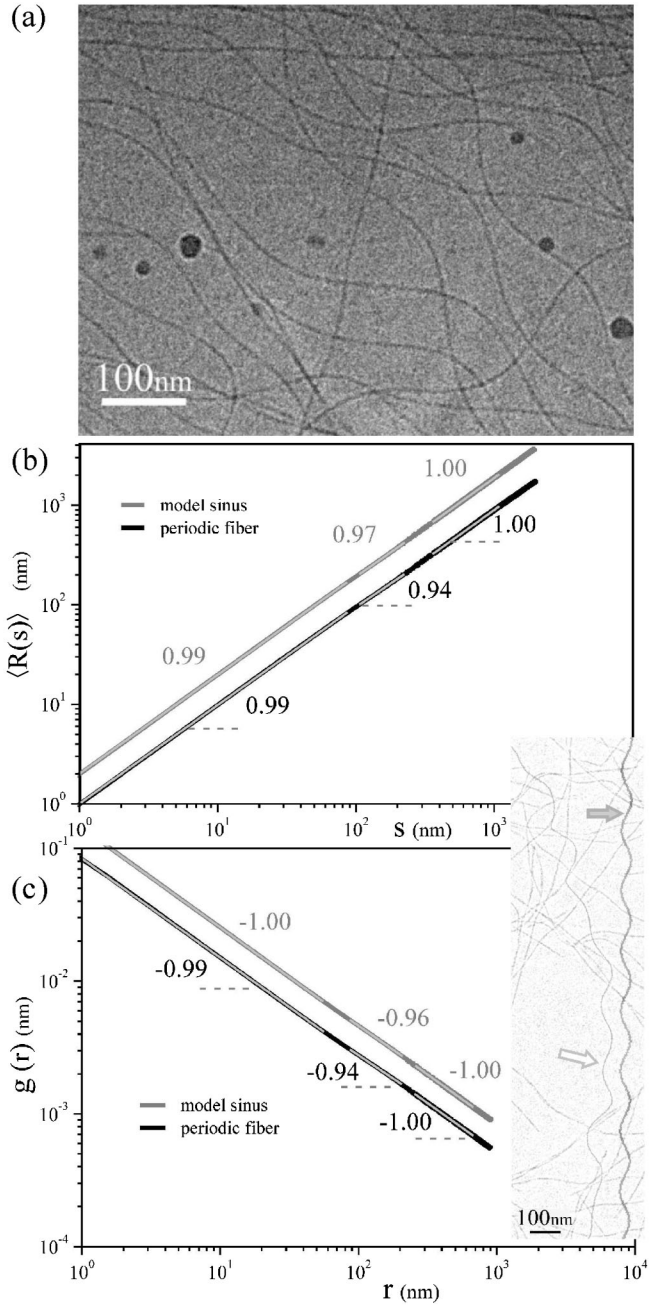

FIG. 2. (a) Cryo-TEM image of lysozyme amyloid fibrils after 2 days incubation at 60 °C and pH 2. Representation in double logarithmic scale of (b) the internal end-to-end distance versus the contour length and (c) the pair correlation function for the real (inset, pointed by white arrow) and a model sinusoid (inset, gray, pointed by gray arrow) fibrils with comparable amplitude and period. The model sinus curve was translated upwards for a better readability in (b) and (c).

TEM inset image, Fig. 2) is compared—at high resolution—with a model sinusoid (pointed by gray arrow in TEM inset image, Fig. 2) of comparable period and oscillation amplitude. Both fibrils show three characteristic scaling regimes in the $\langle R(s)\rangle$ versus s plot of Fig. 2(b). When the contour length is below 100 nm, both fibrils exhibit a pure rodlike behavior with an exponent of 0.99. A different scaling behavior is then discernible at length scales between 150 and 250 nm with $\nu = 0.97$ and 0.94 for the model and real fibrils, respectively. Beyond 500 nm ($\approx 2P$), both fibrils recover an exponent $\nu = 1$. Although the real fibril in the Fig. 2 inset does not develop to sufficiently long contour lengths to identify the asymptotic SAW scaling behavior found in Fig. 1 for longer fibrils, the three scaling regimes in Fig. 2(b) clearly indicate a complex behavior of the lysozyme amyloid fibrils also below L_p. The same evolution is captured in Fig. 2(c) by the pair correlation function $g(r)$ expressing the portion of contour length $s(r)$ contained within a circle of radius r centered in a given point of the fibril and averaged along the fibril [16]:

$$g(r) = \frac{s(r)}{\pi r^2}, \tag{1}$$

where the exponents α found for $g(r) \sim r^{\alpha}$ agree well with those expected by extrapolating $2r \approx \langle R(s)\rangle \sim s^{\nu}$ yielding $\alpha = 1/\nu - 2$.

These fibrils are then well described by four characteristic scaling regimes accounting for: (i) the rigidity of the fibrils for $s < L_b$, with L_b being the characteristic bending length ($L_b \approx 150$ nm); (ii) a characteristic undulation for $L_b < s < P$ ($P \approx 250$ nm); (iii) the rigidity of the undulating fibrils at $P \ll s < L_p$; (iv) the semiflexible behavior of the fibrils following a 2D SAW for $s > L_p$ (Fig. 1).

To characterize further L_b independently from scaling concepts, we apply the wormlike chain model (WLC) at the undulation length scales. In Fig. 3(a), we give the experimental data expressing $\langle R^2(s)\rangle/L_p^2$ versus s/L_p over a period P for the fibril in the inset of Fig. 2(c) ($L_p = 1089$ nm) and we fit the $0 < s < P$ part by the 2D WLC model:

$$\frac{\langle R^2\rangle}{L_p^2} = 4\frac{s}{L_p}\frac{L_b}{L_p}\left(1 - \frac{2L_b/L_p}{s/L_p}\left(1 - e^{-(s/L_p)/(2L_b/L_p)}\right)\right) \tag{2}$$

Equation (2) is the reduced form of the WLC model typically used in semiflexible polymer [22,24] to extract the persistence length, and yields in the present limit the L_b/L_p ratio, corresponding to 0.21 and 0.17 for the model and real fibrils, respectively.

An additional means to estimate L_b is through the decay of the bond correlation function $\langle\cos\theta(s)\rangle$ at short s and by fitting it with the 2D model for semiflexible polymers:

$$\langle\cos\theta(s)\rangle \approx e^{-(s/2L_b)} = e^{-(s/L_p)/(2L_b/L_p)}, \tag{3}$$

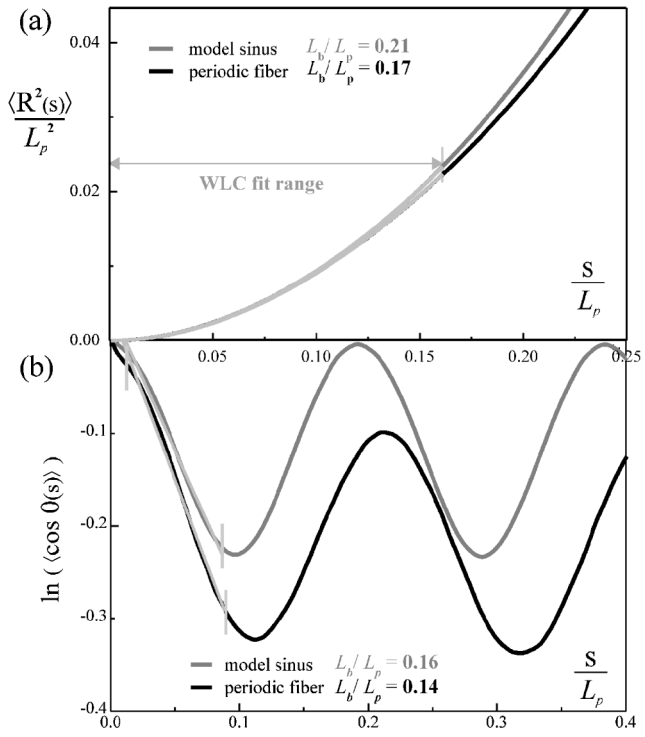

FIG. 3. (a) Reduced squared mean internal end-to-end distance versus reduced contour length for the real and model periodic fibrils. The WLC fit in 2D is plotted in light gray. (b) Logarithm of the bond correlation function versus contour length and exponential decay fit for the real and model periodic fibrils.

where θ is the angle between the tangent vectors to the fibril at two points separated by a contour distance s and the factor 2 is used to rescale the exponential decay to account for the two-dimensional conformation of protein fibrils absorbed on a substrate [11,13,22].

By fitting the data with Eq. (3) at small s/L_p in Fig. 3(b) one finds values of L_b/L_p of 0.16 and 0.14 for the model and real fibrils considered, which are in excellent agreement with values extracted by Eq. (2).

What is the origin of the bending at length scales corresponding to L_b? If these features are a topological reflection of the intrinsic chirality of the fibrils, this could either arise from twisted or helical amyloids. Because twisted amyloid fibrils have a low width-to-thickness ratio, with high Gaussian curvature but no bending curvature [25], only projections of helical amyloid fibrils, with high bending but no Gaussian curvature [25] could be invoked to produce such a wavy feature. However, the presence of typical helical amyloid fibrils here can be easily ruled out: first, the height profile observed (Fig. 4) is not characteristic of the usual helical amyloid profile [26] second, helical amyloids should not be observed for such low width-to-thickness ratio [25–28], and finally, the period-to-width ratios in the present case exceed by 1 order of magnitude that reported for helical fibrils [25–28]. We propose below an alternative possible source of the

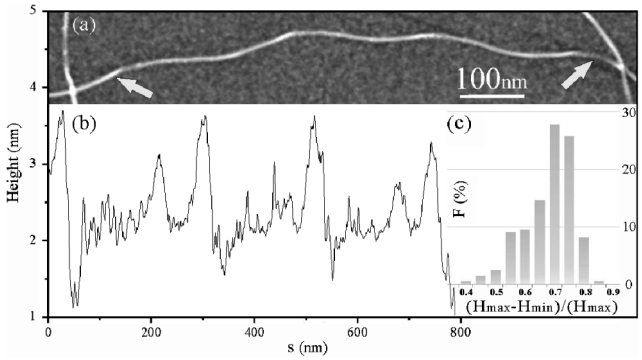

FIG. 4. (a) AFM height image. (b) Height profile along the fibril (section between the arrows). (c) Frequency distribution of normalized cross-section variation measured over 200 fibrils.

observed structural features. The specific bending, occurring at short length scales in the lysozyme fibrils, identified by a characteristic L_b and period P, can be rationalized by considering the variations of the fibrils cross-section orientation along their contour length. Figure 4(a) shows a lysozyme amyloid fibril and Fig. 4(b) shows the corresponding AFM height profile, in which a periodic variation of the height is clearly resolved. These height fluctuations, observed in a systematic way both on mica (Fig. 4) and on graphite (Fig. S4 [23]), have a highly specific profile, with sharp maxima typical of twisting fibrils with a rectangular cross section of width $H_{\max}$ and thickness $H_{\min}$ [Fig. 4(c)]. Orientation variations of the cross section induce periodic changes in the area moment of inertia I of the fibril with respect to the bending plane. Because the persistence length l of a fibril is directly related to the area moment of inertia I via $l = EI/k_BT$ [29], in which E is the Young modulus of the fibril, k_B is the Boltzmann constant and T the temperature, it is obvious that changes in cross-section orientation do affect directly the bending properties along the fibrils. In order to find out whether these fluctuations can sufficiently well explain the observed complex behavior at length scales of the order of L_b, we compare the expected fibril propensity to bend at short and long length scales.

Because the characteristic length scale upon which bending occurs, be this L_b or L_p, is the measure of the energy in k_BT units necessary to bend the fibril, at low enough length scales, bending will occur with the lowest energy mode, that is toward the minimum area moment of inertia $I_{\min}$ and $L_b \approx EI_{\min}/k_BT$ [13]. At large length scales, however, reflecting the real persistence length L_p, the area moment of inertia needs to be averaged [23] and $L_p \approx E(I_{\max} + I_{\min})/2k_BT$ [23,30,31]. Thus, the ratio between the short and long length scale bending features is expected to be of the order: $L_b/L_p \approx 2I_{\min}/(I_{\max} + I_{\min})$. By taking a rectangularlike cross section for the lysozyme amyloid fibrils fluctuating between $H_{\max}$ and $H_{\min}$, with $r \approx H_{\max}/H_{\min} \approx 3.5$ as in Fig. 4(c) [23] one finds that $L_b/L_p \approx 0.15$, which is very close to the corresponding 0.17 and 0.14 ratios observed in Figs. 3(a) and 3(b), respectively.

In summary we have shown that under specific temperature and pH conditions, lysozyme fibrillation leads to an unconventional type of amyloid fibrils in which scaling regimes occur at multiple length scales. As many as three characteristic dimensions are needed to describe the system, corresponding to the bending length, the period of the undulation, and the persistence length of the fibrils, to which four different scaling regimes are associated. These topological features are interpreted to arise from a twisting anisotropic cross-section combined with thermal bending energy.

The authors wish to thank S. Handschin for TEM and cryo-TEM analysis at EMEZ.

*raffaele.mezzenga@agrl.ethz.ch

[1] F. Chiti and C. M. Dobson, Annu. Rev. Biochem. **75**, 333 (2006).
[2] J. P. Taylor, J. Hardy, and K. H. Fischbeck, Science **296**, 1991 (2002).
[3] S. Zhang, Nat. Biotechnol. **21**, 1171 (2003).
[4] F. G. Pearce, S. H. Mackintosh, and J. A. Gerrard, J. Agric. Food Chem. **55**, 318 (2007).
[5] M. Bucciantini *et al.*, Nature (London) **416**, 507 (2002).
[6] M. B. Pepysi *et al.*, Nature (London) **362**, 553 (1993).
[7] A. L. Gharibya *et al.*, J. Mol. Biol. **365**, 1337 (2007).
[8] S. T. Ferreira, M. N. N. Vieira, and F. G. De Felice, IUBMB Life **59**, 332 (2007).
[9] M. R. H. Krebs *et al.*, Protein Sci. **13**, 1933 (2004).
[10] L. N. Arnaudov and R. De Vries, Biophys. J. **88**, 515 (2005).
[11] K. Rechendorff *et al.*, J. Chem. Phys. **131**, 095103 (2009).
[12] F. Valle *et al.*, Phys. Rev. Lett. **95**, 158105 (2005).
[13] J. Adamcik *et al.*, Nature Nanotech. **5**, 423 (2010).
[14] P. A. Rühs *et al.*, Soft Matter **7**, 3571 (2011).
[15] S. Bolisetty, J. Adamcik, and R. Mezzenga, Soft Matter **7**, 493 (2011).
[16] P. G. de Gennes, *Scaling Concepts in Polymer Physics* (Cornell University Press, Ithaca, 1979).
[17] M. Rubinstein and R. H. Colby, *Polymer Physics* (Oxford University Press, New York, 2003).
[18] R. Diaz-Avalos *et al.*, Proc. Natl. Acad. Sci. U.S.A. **102**, 10 165 (2005).
[19] J. Jiménez *et al.*, J. Mol. Biol. **311**, 241 (2001).
[20] S. Jordens *et al.*, Biomacromolecules **12**, 187 (2011).
[21] A. Relini *et al.*, Biophys. J. **98**, 1277 (2010).
[22] G. Witz *et al.*, Phys. Rev. Lett. **101**, 148103 (2008).
[23] See Supplemental Material at http://link.aps.org/supplemental/10.1103/PhysRevLett.107.238101 for AFM, TEM, cryo-TEM, height, pH, and area moment of inertia analysis.
[24] C. Rivetti, M. Guthold, and C. Bustamante, J. Mol. Biol. **264**, 919 (1996).

[25] Y. Sawa *et al.*, Proc. Natl. Acad. Sci. U.S.A. **108**, 6364 (2011).
[26] J. Adamcik *et al.*, Angew. Chem., Int. Ed. **50**, 5495 (2011).
[27] C. Lara *et al.*, Biomacromolecules **12**, 1868 (2011).
[28] L. Ziserman *et al.*, Phys. Rev. Lett. **106**, 238105 (2011).
[29] G. S. Manning, Phys. Rev. A **34**, 4467 (1986).
[30] C. Sachse, N. Grigorieff, and M. Fändrich, Angew. Chem., Int. Ed. **49**, 1321 (2010).
[31] J. Smith *et al.*, Proc. Natl. Acad. Sci. U.S.A. **103**, 15 806 (2006).